scientific reports

Check for updates

OPEN

Comparative evaluation of collagen modifications in breast cancer in human and canine carcinomas

Ana Paula Vargas Garcia[1], Luana Aparecida Reis[2], Bárbara Regina Melo Ribeiro[2], Cristiana Buzelin Nunes[3], Ana Maria de Paula[2,4]✉ & Geovanni Dantas Cassali[1]

New diagnostic and therapeutic approaches have been increasingly demanded due to the high morbidity and mortality associated with breast cancer. Recently, changes in the collagen fibres in mammary neoplasms have been shown to provide information that can be helpful for more accurate diagnosis. We aimed to conduct a comparative analysis of the tumour stroma in human and canine mammary neoplasms to assess the relationship between collagen modifications and the behaviour of carcinomas in both species, by multiphoton microscopy. We present a retrospective study of 70 cases of human mammary tumour and 74 cases of canine mammary tumour. We analysed sections stained with haematoxylin and eosin from 1,200 representative areas of normal mammary tissue, fibroadenoma, grade I invasive carcinoma, grade III invasive carcinoma and invasive micropapillary carcinoma in human species and 1,304 representative areas of normal mammary tissue, benign mixed tumour, mixed carcinoma, carcinosarcoma, invasive micropapillary carcinoma and solid carcinoma in canine species. We obtained that both human and canine mammary carcinomas present lower density of collagen fibres, higher density of cells and the collagen fibres are more aligned than in normal tissue. For human mammary carcinomas, the collagen fibres are more linear as compared to normal tissue. In addition, we demonstrated that the carcinomas with unfavourable prognosis present shorter collagen fibres, and these collagen changes correlate with the clinical and pathological data in human and canine species. For dogs, there is a correlation between the mean fibre length with the specific survival times. Thus, we demonstrate that dogs provide an excellent comparative perspective for studying how changes in the tumour stroma affect patient survival.

Keywords Collagen fibre, Collagen alignment, Tumour microenvironment, Breast cancer, Matrix remodelling, Tumour-associated stroma

Mammary gland neoplasms are characterized by collagen deposition, remodelling, and linearisation of the extracellular matrix, leading to fibrosis that promotes malignancy[1,2]. The stiffened stroma enhances tumour cell growth, survival, and migration, driving an epithelial-mesenchymal transition. A rigid stroma also induces angiogenesis, hypoxia, and compromises antitumour immunity[3]. It is a well-established fact that the tumour microenvironment, also known as the tumour-associated stroma, is composed of a diverse combination of non-tumour cells, such as fibroblasts, macrophages and other immune cells, vascular cells, adipocytes, and others, in addition to the extracellular matrix. Studies demonstrated that tumour-associated stroma plays a key role in the initiation and progression of a wide variety of neoplasms, having multiple roles in tumour biology[4,5]. Collagen, specifically, plays a crucial role in metastasis development in breast cancer, as well as in matrix metalloprotease activity, that has been the subject of a considerable number of planned and therapeutic studies of many types of cancer[6–9] and specifically in breast cancer[10–18]. It has been shown that the neoplastic mammary glands present more organized and defined collagen fibres when compared to the healthy breast. Therefore, collagen organization is correlated with unfavourable prognosis[1,15–21]. Furthermore, changes in collagen density and fibre organization were associated with tumour grade and overall survival in human[15] and canine[18] breast carcinomas.

[1]Department of General Pathology, Institute of Biological Sciences, Federal University of Minas Gerais, Av. Pres. Antônio Carlos, 6627, Pampulha, Belo Horizonte 31270-901, MG, Brazil. [2]Department of Physics, Institute of Exact Sciences, Federal University of Minas Gerais, Av. Pres. Antônio Carlos, 6627, Pampulha, Belo Horizonte 31270-901, MG, Brazil. [3]Department of Anatomic Pathology, Faculty of Medicine, Federal University of Minas Gerais, Av. Prof. Alfredo Balena, 190, Santa Efigênia, Belo Horizonte 30130-100, MG, Brazil. [4]Present address: Institute of Physics "Gleb Wataghin", University of Campinas, Campinas, SP, Brazil. ✉email: ana@fisica.ufmg.br

Neoplasms naturally developed in domestic dogs have increasingly been used as a valuable source of information to better understand the biology of breast cancer development in women. The canine species presents pathophysiological similarities with the human species and can help in research for new diagnoses and therapies related to this neoplasm[22–28]. The field of comparative oncology aims to approach some existing research deficiency, broadening its focus from classic rodent models to spontaneous tumours that develop in animals. This additional perspective is perceived as a chance to complement and improve the understanding of complex diseases, such as cancer, in relation to tumour development, risk factors and mechanisms of tumourigenesis. Due to the many similarities shared between dogs and humans, the domestic dog has been considered one of the best examples of comparative oncology[21,22,25,26,28–30]. Thus, the aim of this study was to carry out a comparative analysis of the tumour stroma in human and canine mammary neoplasms to evaluate the links between changes in collagen fibres and the behaviour of carcinomas in both species. The study was based on morphological, clinicopathological, immunophenotypic data and imaging by second harmonic generation (SHG) and two-photon excited fluorescence (TPEF) microscopy in cases of human mammary and canine mammary tumour.

Materials and methods

Case selection

This retrospective study involved the analysis of 70 cases of human mammary neoplasms, 74 samples of canine mammary tumours, 20 healthy samples of human mammary tissue, and 12 healthy samples of canine mammary tissue. The canine mammary tissue samples were obtained from the archives of the Comparative Pathology Laboratory at the Federal University of Minas Gerais (UFMG), Brazil. The human mammary tissue samples were collected from the biopsy sector archives of the Faculty of Medicine at the Federal University of Minas Gerais (UFMG), Brazil. Both the canine and human samples were sourced from naturally occurring tumours in patients undergoing treatment at the UFMG Veterinary Hospital and the UFMG Hospital das Clínicas. Healthy canine mammary tissue samples were acquired from mammary tissues without mammary chain abnormalities received at the Comparative Pathology Laboratory. Healthy samples of human breast tissue were obtained from breast reduction surgeries performed at the Hospital das Clínicas of UFMG. The selection process encompassed samples with comprehensive information regarding tumour size, presence or absence of regional or distant metastasis, and histological grade.

The two-photon microscopy images were performed on histological slides stained with haematoxylin and eosin (H&E). The slides were prepared using sections of healthy or neoplastic mammary tissue sourced from biopsies involving procedures such as setorectomy, simple mastectomy, or unilateral/bilateral radical mastectomy, determined by factors including tumour size, tumour site, lymphatic involvement, and clinical stage. The selected canine samples were collected between 2009 and 2020 and submitted to histological classification according to the Classification and Grading of Canine Mammary Tumors[31,32] and Consensus for the Diagnosis, Prognosis and Treatment of Canine and Feline Mammary Tumours[33–36]. The selected human samples were collected from 2010 to 2020 a were classified histologically based on the criteria described in the World Health Organization[37]. For correlations between collagen fibre organization parameters, number, waviness and mean fibre length, collagen density and cell density and patient-specific survival, only data from patients treated with surgery alone were included. Score 1 was assigned to patients who died from breast cancer and 0 to living patients. Patients who died for reasons other than mammary cancer were not included.

The canine sample study was performed in view of the fundamental ethical principles under law no. 11.794, of October 8, 2008 and of decree no. 6.899 of July 2009, and with the rules issued by the National Council for the Control of Animal Experimentation (CONCEA) and the international Animal Research: Reporting of In Vivo Experiments (ARRIVE). All experimental protocols were approved by the "Ethics Committee on the Use of Animals" at UFMG, under number 83/2021.

The research on human tissue sample was previously approved by the "Research Ethics Committee" at UFMG (COEP-UFMG) under No. 43947521.3.0000.5149/2021. All experiments were carried out in accordance with the Declaration of Helsinki. As a retrospective study, performed on archive histopathological slides, the need for informed consent from all subjects and/or their legal guardian(s) was waived by the COEP-UFMG.

Performing immunohistochemistry

Histological sections, measuring 4 µm thick, were prepared for immunohistochemical analysis. A commercial anti-mouse/anti-rabbit detection kit (Novolink Polymer Detection System, Leica Biosystems, Newcastle Upon Tyne, United Kingdom, REF RE7158, LOT 6092583), was used following the manufacturer's instructions. Antigen retrieval for estrogen receptor (ER), progesterone receptor (PR), Ki67 and HER2 was performed using steam heat (*Pascal*®) with citrate pH 6.0 (Invitrogen by Thermo Fisher Scientific, 10X low pH, REF 00-4955-58, LOT 2410220, Life Technologies' Corp., 5781 Van Allen Way, Carlsbad, CA92008). The histological sections were incubated with the corresponding primary antibodies for 1 h in a humid chamber at 4 °C. Primary antibodies used included ER (Dako Cat# ER-14-0481, RRID: AB_1545347, goat anti-human EP1 receptor, PTGER1 antibody, unconjugated, LOT 11303512, REF IR084, ready-to-use), PR (LSBio LifeSpan Cat# LS-C26712, RRID: AB_2283822, progesterone receptor (PGR) mouse monoclonal (hPRa2 + hPRa3) antibody, anti-human/mouse/rat, unconjugated, LOT XI3703736, REF MA512642, 0.4 mg/mL, 1:50), HER2 (Dako Cat# AP7629e, RRID: AB_2262284, rabbit anti-human HER2, polyclonal antibody, unconjugated, REF A0485, LOT 00060381, 0.50 g/mL, 1:200), and Ki67 (Thermo Fisher Scientific Cat# MA5-31796, RRID: AB_2787419, mouse anti-human MIB1 receptor, 2A7B1 antibody, unconjugated, LOT 20067572, REF M7240, 46 mg/mL, 1:50). Immunoreactivity was visualized using 3,3'-diaminobenzidine chromogen (Novolink Polymer Detection System, Leica Biosystems, Newcastle Upon Tyne, United Kingdom, REF RE7158, LOT 6092583) and counterstained with Mayer's haematoxylin. Positive controls for the reactions consisted of fragments of canine and human mammary tissues positive for HER-2, ER, PR and Ki67. The primary antibody was omitted and chromogen was added to both

for negative controls. The evaluation of the slides, the quantification of immunoreactive and the classification of immunophenotypes were carried out in accordance with the World Health Organization[32] guidelines (for human samples) and the criteria established by Nunes et al.[33] (for dog samples). The antibodies used were standardized in our laboratory routine, and their antigenic specificity was confirmed through our own research and by reference to others published studies[33–38].

Image acquisition and analyses

The imaging system employed in this study combined SHG and TPEF imaging using a custom setup comprising an Olympus FV300 confocal scanning laser unit connected to a BX61- upright microscope. The SHG images allow to extract information from the collagen fibres and the TPEF allows to extract details of the cell arrangements in the tissue. Details of the image acquisition methodology is described in our previous publications[17,18,39]. In brief, we used 140 fs pulses centred at the wavelength of 800 nm. The beam is focused on the sample microscope slab by a 20X objective with a high numerical aperture (NA = 0.9) and the images are obtained in back scattering geometry. The SHG is measured at 400 nm using a filter with bandwidth of 20 nm by directing the signal to a non-descanned detector placed just above the objective. The fluorescence signal from the eosin dye staining the tissue is measured by the standard de-scanned detector of the confocal unit at the wavelength band of 560 to 600 nm. The transmitted laser image is also collected by the condenser of the microscope. We measured images at the optimized focus position and at ± 1 µm from this position to allow for noise filtering by the software. The images were acquired for areas of 0.47×0.47 mm2. For human samples, 1,200 representative sections of normal human breast tissue (NMTh) and evaluated human histological types were chosen from H&E-stained slides. For canine samples, 1,304 representative sections of normal mammary tissue (NMTc) and canine histological types evaluated from sections stained with H&E were defined. In cases where histological slides included normal mammary regions, images of the 10 most representative areas in human and canine samples were captured. Regarding neoplastic tissues, 10 to 15 highly representative intratumoural regions were selected for measurements. SHG and TPEF signals from selected areas were measured for further analyses. Additionally, brightfield microscopy images of H&E-stained tissue were acquired from the same measured areas using the Olympus BX41 microscope coupled to the *SPOT Insight Color* camera for comparative purposes. The capture software used was *SPOT Advanced*.

Our quantitative analyses of collagen fibre and cell segment parameters utilized PyFibre, an open-source software package (Python Fibrous Image Analysis Toolkit), that we specifically designed for automated segmentation of images into cellular and collagen regions, allowing extraction of pertinent parameters. PyFibre is openly accessible on GitHub[40]. During the analyses process, the integration of SHG and TPEF signals along with laser transmission data was employed to improve the accurate identification of collagen fibres and cellular features in the images. This approach utilized the TPEF and SHG signals, in addition to a copy of the laser transmission data, to better discern collagen fibres and cellular features in the images. Data were extracted and analysed according to Reis et al.[17], Garcia et al.[18] and Gomes et al.[39].

Statistical analysis

The Shapiro-Wilk test was employed to assess normality in small sample groups, while the Kolmogorov-Smirnov test was used for larger sample groups. Due to the non-parametric nature of the data, the Kruskal Wallis test and the Dunn test were performed for multiple comparisons of the medians between groups. We employed Spearman's Correlation Coefficient and linear regression statistical tests to establish correlations between clinicopathological data of patients and collagen fibre parameters. The cancer-specific survival rate was estimated using the Kaplan–Meier curve, and the comparisons between groups were performed using the Mantel-Cox log rank test. To evaluate the independence or association between the categorical variables mean fibre length and histological grading, clinical staging, cell proliferation and significant molecular subtype between categorical variables using the chi-square test and Fisher's Exact Test. The graphs were presented in contingency graphs. These analyses were performed using *Prism* (version 8.0, GraphPad, San Diego, CA, United States). A value of $p < 0.05$ was considered statistically significant for all analyses. The p values less than 0.001 are denoted by (***), p less than 0.01 are denoted by (**) and p less than (0.05) are denoted by (*).

Results

Details of the analysed samples

Table 1 presents the details of the histological subtypes analysed, number of samples, patient age, clinical staging, histological grading, molecular subtype and survival information for human breast neoplasms. Table 2 provides equivalent details for canine mammary neoplasms. The analysis of correlations between collagen fibre parameters and clinicopathological data did not include Fibroadenoma (Fb) in women and benign mixed tumours (BMT) in dogs. It should be noted that the canine data presented in this article comprise a different data set from that used in our previously published works. Importantly, there is no overlap between the samples included in this study and those analysed in our previous publications[18,41]. For this study, we selected more recent cases, ensuring a more accurate assessment of potential changes in the genetic, environmental, and social conditions of the animals involved. Additionally, we prioritised cases with comprehensive descriptions of clinical-pathological data, which allowed us to deepen the analysis of additional prognostic factors. Nonetheless, due to the low occurrence of carcinosarcomas in clinical practice, we used some of the same carcinosarcoma cases described in our previous publication[18]. However, all the other cases selected are new, and the analyses performed in this work are original, providing new insights into tumour progression.

The women were followed up for a minimum of 05 years and a maximum of 10 years. At the conclusion of the study, we completed the follow-up of 43 patients. Of these, 06 women had died and 37 were still alive. Follow-up was not possible for 11 patients. The distribution of women based on clinical staging was as follows: 04 women

Histological type	*n*	Age (year)	Staging (TNM)					Histological grades			Molecular subtype				Survival (months)
			I	II	III	IV	V	I	II	III	HR+/ Ki67 < 20%	HR+/ Ki67 > 20%	HR+/- HER2+	HR-/ HER2-	
Fb	12	34.2	NA	NA	NA	NA	NA	NA	NA	NA	NA	NA	NA	NA	NA
TC	4	71.3	2	2	0	0	0	4	0	0	4	0	0	0	66.0
ICgI	16	68.4	5	7	0	3	1	16	0	0	13	3	0	0	86.3
ICgIII	21	59.6	5	2	2	10	2	0	0	21	2	12	4	3	79.1
IMC	17	52.3	4	3	1	9	0	3	8	2	3	8	6	0	59.5
Total	**70**	-	**16**	**14**	**3**	**22**	**3**	**23**	**8**	**23**	**22**	**23**	**9**	**4**	-

Table 1. Clinicopathological features of human mammary neoplasms. For the age and the survival, the data are the mean values with the standard deviation in brackets. Fibroadenoma (Fb), tubular carcinoma (TC), grade I invasive carcinoma (ICgI), grade III invasive carcinoma (ICgIII), invasive micropapillary carcinoma (IMC). N = number of cases. NA = not evaluated. HR = hormonal receptor.

Histological type	*n*	Age (year)	Staging (TNM)					Histological grades			Molecular subtype				Survival (days)
			I	II	III	IV	V	I	II	III	HR+/ Ki67 < 20%	HR+/ Ki67 > 20%	HR+/- HER2+	HR-/HER2-	
BMT	15	10	NA	NA	NA	NA	NA	NA	NA	NA	NA	NA	NA	NA	NA
MC	14	11	7	3	4	0	0	11	2	1	13	1	0	0	1116.2
CS	6	8.5	0	0	4	0	2	0	0	6	2	4	0	0	321.8
IMC	16	10.8	0	1	2	10	3	2	9	5	1	7	3	5	293.9
SC	23	11.8	5	4	4	9	1	2	10	11	3	17	2	1	279.5
Total	**74**	-	**12**	**8**	**14**	**19**	**6**	**15**	**21**	**23**	**19**	**29**	**5**	**6**	-

Table 2. Clinicopathological features of canine mammary neoplasms. For the age and the survival, the data are the mean values with the standard deviation in brackets. Benign mixed tumour (BMT), mixed carcinoma (MC), invasive micropapillary carcinoma (IMC), carcinosarcoma (CS), solid carcinoma (SC). N = number of cases. NA = not evaluated.

with TC (02 alive, 02 not followed up), 16 women with ICgI (01 died, 14 alive, 01 not followed up), 21 women with ICgIII (18 alive, 03 not followed up), and 17 women with IMC (05 died, 09 alive, 03 not followed up). All patients had complete information on clinical staging.

The female dogs were followed up for a minimum of 02 years and a maximum of 05 years. At the conclusion of the study, we completed the follow-up of 55 bitches. Of these, 46 patients had died and 09 were still alive. Follow-up was not possible for 04. The distribution of patients based on clinical staging was as follows: 14 patients with MC (07 died, 07 alive), 16 with IMC (14 died, 02 not followed up), 06 with CS (all died), and 23 with SC (19 died, 02 alive, 02 not followed up). Three patients with IMC did not have complete information to define the clinical staging. Women with Fb and dogs with BMT were not followed up.

Images and extract parameters

Figure 1 present representative images of the human histological sections studied to illustrate the imaging procedure. The histological types in the columns are indicated as NMTh (Fig. 1A, E, I and M), Fb (1B, 1 F, 1 J and 1 N), ICgI (1 C, 1G, 1 K and 1O) and IMC (1D, 1 H, 1 L, 1P) for the normal mammary gland, fibroadenoma, grade I invasive carcinoma and invasive micropapillary carcinoma, respectively. The fourth row presents images of individual fibres, displayed in varying colours, extracted using our image analysis methodology (1M-1P). The SHG signal is from the collagen fibres, that are non-centrosymmetric fibres, and the TPEF signal corresponds to the fluorescence emission of the dye eosin. The SHG and TPEF represent false colour representations of normalized intensity maps to accentuate various features. Comparing the two images allows to segment the tissue into collagen and cellular regions, and thus extract quantitative parameters. The images of the extracted collagen fibres are presented in Fig. 1M and N 1O 1P. For the canine samples, the methodology for acquiring the images and extracting the parameters has already been thoroughly exemplified in previous articles[17,18,39]. More details about measurements and image analyses can be found in the 'Materials and Methods' section.

Human mammary tissue (NNMTh, Fig. 1) is composed of lobes, ducts, and an interconnected network of connective tissue (indicated by the asterisk in Fig. 1A). connective tissue, abundant collagen fibres are found surrounding the parenchyma, which exhibit different orientations within the breast tissue (Fig. 1E). In benign neoplasms of the mammary gland, such as fibroadenoma (Fb) in women (Fig. 1B), and also benign mixed tumours (BMT) in dogs, an abundance of collagen fibres is visible in the adjacent connective tissue, exhibiting a pattern of diverse orientation similar to that of NNMTh (Fig. 1F) and NMTc. However, in grade I invasive carcinoma (ICgI) and invasive micropapillary carcinoma (IMC), there is a reduction in collagen density and collagen fibres are organized in a preferential direction (Fig. 1G, H, O and P). ICgI has a favourable prognosis, while IMC is associated with an unfavourable prognosis[31,32,35]. Mixed carcinomas (MC) originates from the malignant transformation of benign mixed tumours, presenting a complex histological pattern and favourable prognosis[31–36,42,43]. On the other hand, carcinosarcoma (CS) is characterized by the coexistence of malignant epithelial and mesenchymal components, presenting an extremely aggressive biological behaviour, with a high incidence of metastases to regional lymph nodes and lower overall survival[29,31,34,36]. In IMC and SC, decrease in collagen density and an increased alignment of collagen fibres in the surrounding connective tissue are also noticeable.

Our image analysis and fibre and cell extraction procedures allowed the quantification of many of these microscopic features described. Collagen fibre organization parameters (fibre segment SHG coherence), number of collagen fibres (no. fibres), mean fibre length, collagen density (fibre segment coverage) and cell density (cell segment coverage) for all histological types of human and canine mammary neoplasms and for NMTh and NMTc that are presented in Fig. 2.

Carcinomas present aligned fibres, lower fibre density and higher cell density

The collagen fibre organization parameter assesses the degree of alignment of collagen fibres within the tissue, with values spanning from zero (indicating a random arrangement) to one (indicating highly oriented and aligned fibres along a specific direction). As depicted in Fig. 2A human mammary carcinomas exhibit a greater degree of collagen fibre alignment when compared to NMTh. Canine neoplastic tissues exhibit the same behaviour (see Supplementary Fig. S1). These results clearly delineate a distinction between normal and carcinomatous tissue in both species.

Figure 2B show the waviness of the collagen fibres for human mammary tissues. This parameter evaluates the straightness of the collagen fibres extracted from the stromal regions, where 1 means perfectly linear fibres and 0 means perfectly wavy fibres. In human mammary tissues, carcinomas present more linear fibres compared to NBTh and Fb. In canine mammary tissue (see Supplementary Fig. S1), it was not possible to verify this same behaviour. We observed that none of the histological types present statistically significant differences with NBTc. SC has more linear collagen fibres compared to BMT and ICM, and CS has more linear fibres compared to BMT and IMC.

The number of collagen fibres, the fibre coverage area and the cell coverage area determine the collagen density and cell density in the measured regions. These are important parameters to evaluate changes related to the stromal and epithelial components of human (Fig. 2C and E) and canine (see Supplementary Fig. S1) mammary carcinomas. Figure 2C and D show that the number of collagen fibres and the area covered by fibres decrease in carcinomas compared to NMTh and neoplastic tissues benign. Comparatively, Fig. 2E show that carcinomas present a larger area covered by cells compared to NMTh and benign neoplastic tissues. We observed similar behaviour in the canine species (see Supplementary Fig. S1), however we did not observe significant differences in the number of collagen fibres, area covered by fibres and area covered by cells between CS with NMTc and BMT.

Furthermore, the collagen fibre length is an important parameter for evaluating the stromal changes that occur in neoplastic mammary tissues[1,9,18,44]. Figure 2 F show that the mean fibre length is different between

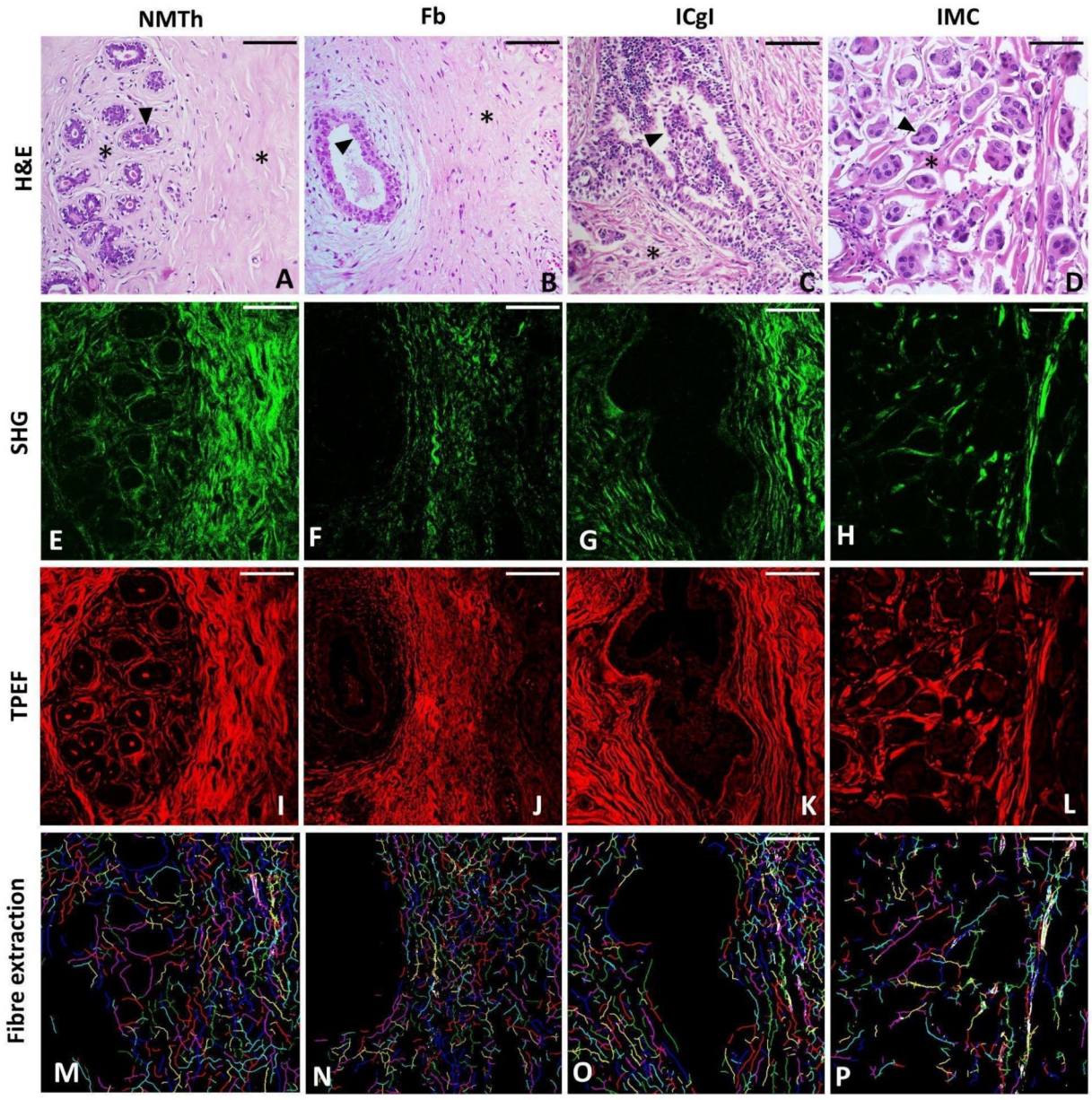

Fig. 1. Acquired images (20X objective). The optical microscopy H&E (**A**-**D**), second harmonic generation microscopy (**E**-**H**), two-photon excited fluorescence microscopy (**I**-**L**) and the extracted collagen fibres with each fibre in a random colour (**M**-**P**) for the human normal mammary tissue (**A**, **E**, **I** and **M**), fibroadenoma (**B**, **F**, **J** and **N**), grade I invasive carcinoma (**C**, **G**, **K** and **O**) and invasive micropapillary carcinoma (**D**, **H**, **L** and **P**). Asterisk HE: stroma. HE arrowhead: epithelial cells. The scale bar is 100 μm.

the histological types in humans. Carcinomas with favourable prognosis (TC and ICgI) present a higher mean fibre length as compared to carcinomas with unfavourable prognosis (ICgIII and IMC). In canine mammary carcinomas, we identified the same behaviour (see Supplementary Fig. S1 online). Carcinoma with favourable prognosis (MC) presents the highest average fibre length as compared to carcinomas with reserved to unfavourable prognosis (CS, IMC and SC).

More aggressive carcinomas present lower fibre density, higher cell density and shorter collagen fibres

To evaluate the influence of the tumour stroma on the behaviour of human and canine mammary carcinomas, we verified whether the density of collagen fibres, cell density and fibre length correlate with the clinicopathological data. Immunohistochemistry was performed on a sample of 58 human and 59 canine mammary tissue samples, all diagnosed with mammary carcinoma. Figure 3 shows these correlations. Here, the increased aggressiveness

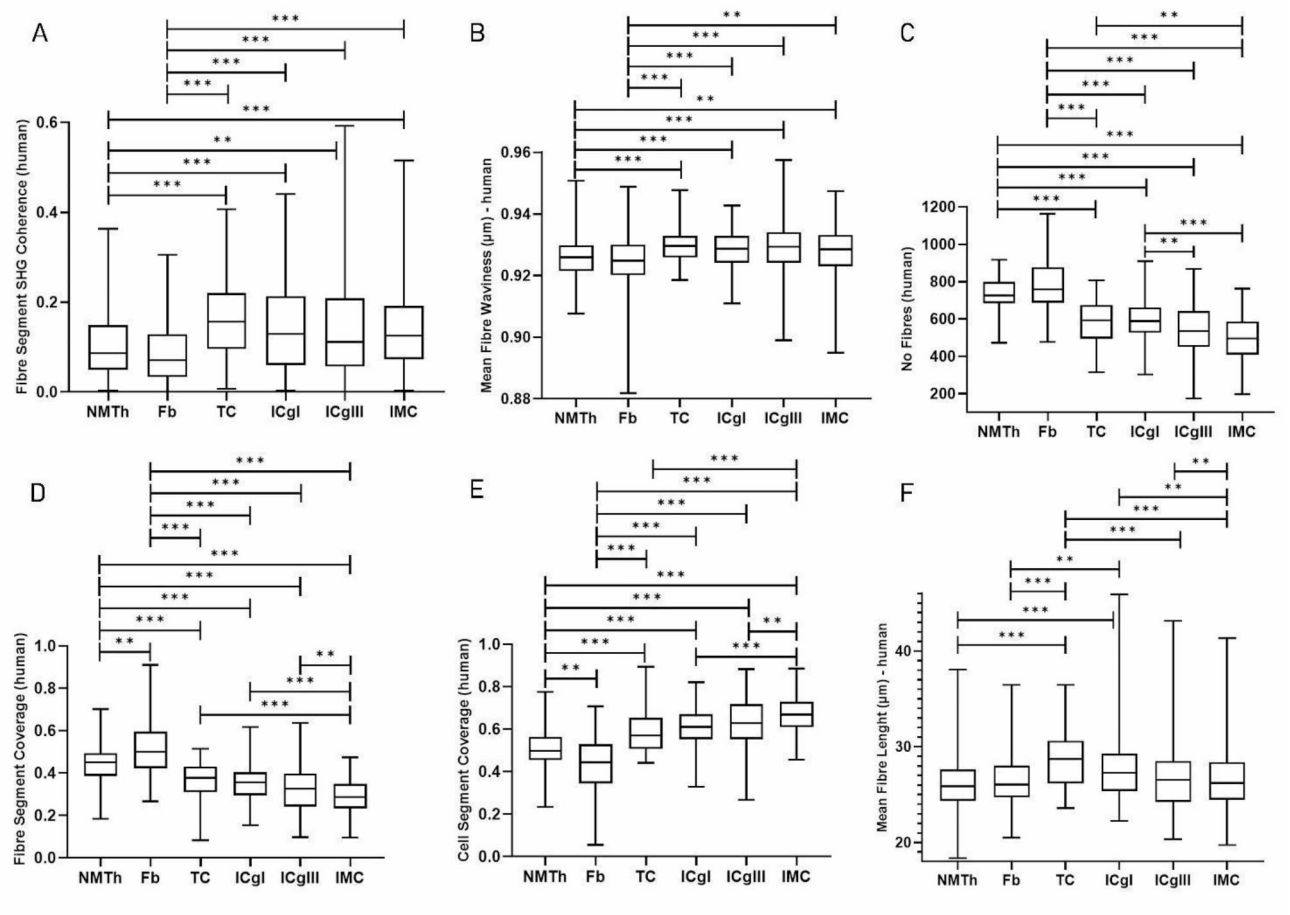

Fig. 2. Parameters of the human mammary gland analysed by second harmonic generation and two-photon excited fluorescence techniques. Kruskal Wallis test and the Dunn test. Boxplot graphics showing the calculated parameters for the fibre segment SHG coherence, mean fibre waviness, mean fibre length, number of fibres, fibre segment coverage and cell segment coverage for human normal mammary tissue (NMTh, $n=20$), fibroadenoma (Fb, $n=12$), tubular carcinoma (TC, $n=04$), invasive carcinoma grade I (ICgI, $n=16$), invasive carcinoma grade III (ICgIII, $n=21$), invasive micropapillary carcinoma (IMC, $n=17$) in human samples ($n=90$). The centre lines show the medians, the box limits indicate the 25th and 75th percentiles, the whiskers extend 1.5 times the interquartile range from the 25th and 75th percentiles and the outliers are represented by dots. The p values less than 0.001 denoted by (***), p less than 0.01 are denoted by (**) and p less than (0.05) are denoted by (*).

of carcinomas was associated with cases that presented the following characteristics: higher histological grade, larger probability of developing local and/or distant metastases, higher rate of cellular proliferation and larger probability of presenting molecular expressions of the "triple-negative" and "Her2 overexpressed". For the correlations, the cell proliferation rate was obtained from the Ki67 count and the molecular subtype of human and canine mammary carcinomas were categorized as follows: 1 for luminal A (positive hormone receptors, negative HER-2 and proliferative rate less than 20%), 2 for luminal B (positive hormone receptors, negative HER-2 and proliferative rate greater than 20%), 3 for HER-2 positive (positive or negative hormone receptors and positive HER-2 independent of the proliferative rate) and 4 for triple negative (negative hormone receptors, negative HER2 regardless of proliferative rate).

We note that the mean fibre length inversely correlates with histological grade (Fig. 3A and B), clinical staging (Fig. 3C and D), cell proliferation (Fig. 3E and F) and molecular subtype (Fig. 3G and H) in women and dogs. Here, we show data correlating the increased tumour aggressiveness with the smaller collagen mean fibre length. It is important to note that while human molecular subtypes have been adapted for use in canine mammary carcinomas, their prognostic value in dogs remains controversial, particularly for HER2 overexpression. Conflicting results in the literature have made it difficult to establish a consistent correlation between HER2 status and clinical outcome in dogs. Despite this limitation, we found that mean fibre length inversely correlates with histological grade (Fig. 3A and B), clinical staging (Fig. 3C and D), cell proliferation (Fig. 3E and F) and molecular subtype (Fig. 3G and H) in both women and dogs. Here, we show data correlating the increased tumour aggressiveness with the smaller collagen mean fibre length.

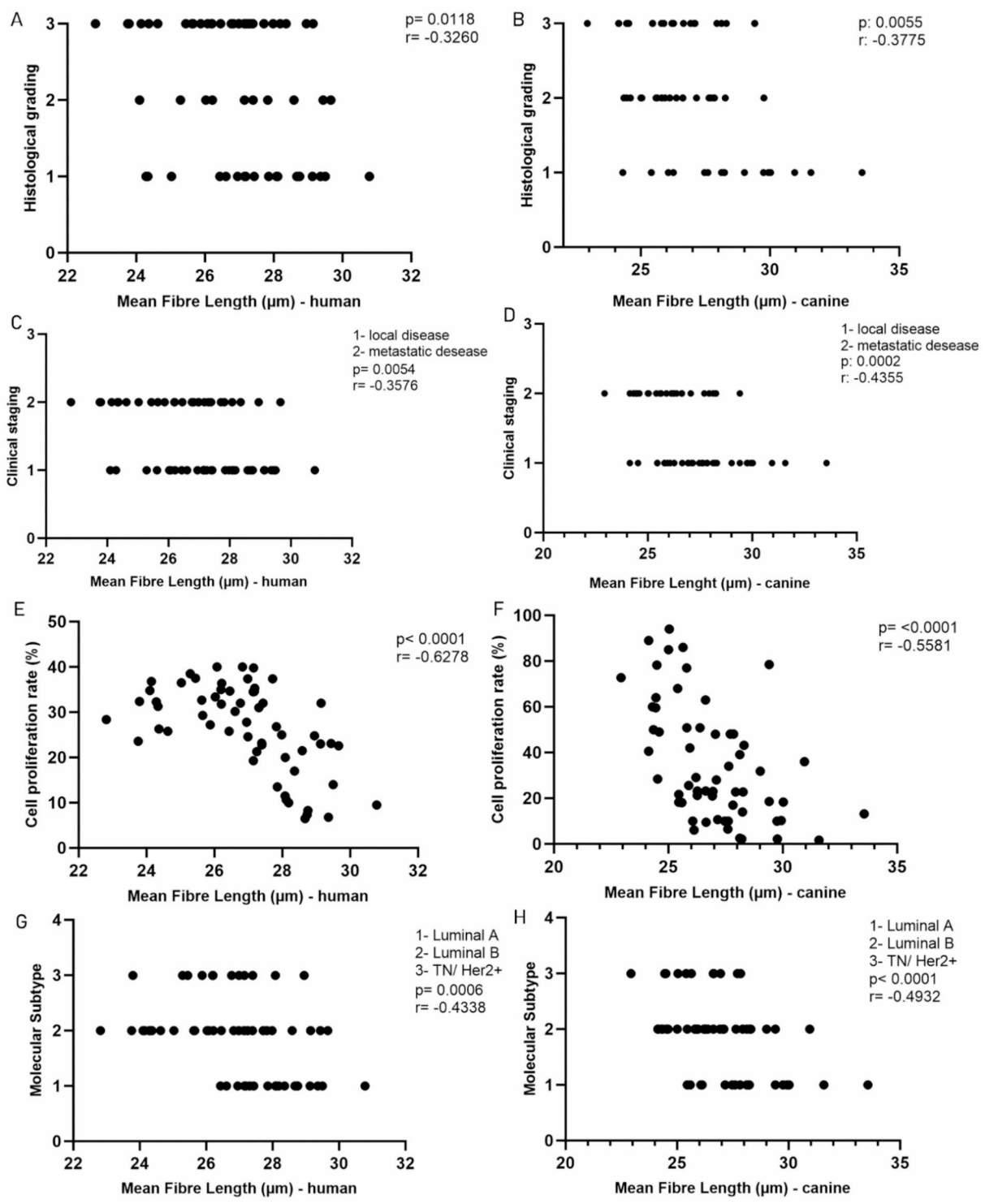

Fig. 3. Correlation between clinicopathological parameters and mean fibre length in women and dogs. Spearman's correlation between histological grading and mean fibre length in women (**A**, $n=58$) and dogs (**B**, $n=59$). Spearman's correlation between clinical standing and mean fibre length in women (**C**, $n=58$) and dogs (**D**, $n=59$). Linear regression between cell proliferation and mean fibre length in women (**E**, $n=58$) and dogs (**F**, $n=59$). Spearman's correlation between molecular subtype and mean fibre length in women (**G**, $n=58$) and dogs (**H**, $n=59$).

To determine the influence of mean fibre length on patient survival, we established a cut-off point disregarding histological subtype, histological grade, clinical staging, cell proliferation rate and molecular subtype. For this, the data were organized in ascending order and the median fibre length value was calculated. Therefore, the value 27 µm was determined as the cut-off point, categorizing patients into two groups based on this cut-off point. Those diagnosed with carcinomas with fibres smaller than 27 µm were grouped in the first category, while those with carcinomas with collagen fibres larger than 27 µm were grouped in the second category. We assigned 0 to patients alive at the end of the study and 1 to patients who died from mammary carcinoma. For those diagnosed with carcinomas with collagen fibres larger than 27 µm (represented by the red line), the average survival was 150 days. On the other hand, patients with carcinomas with fibres larger than 27 µm (shown by the blue line) had a median survival of 849 days. Notably, more aggressive carcinomas with an unfavourable prognosis had shorter collagen fibres compared to less aggressive carcinomas with a favourable prognosis. In Fig. 4A, we show survival curves for dogs. We extend this method to define cut-off points for SHG coherence, mean fibre waviness, number of fibres, fibre segment coverage, and cell segment coverage. However, no significant correlations were observed between these metrics and dog-specific survival. These findings support the data from our current study and are in line with our previously published work[18]. It should be noted that the canine dataset examined in this study differs from our previous assessment.

In humans, it was not possible to establish a specific survival curve for cancer using the same methodology as used for dogs. This is because approximately 85% of the patients in the study are alive and still under medical supervision. Thus, the median survival was not reached in any of the stratified groups, making it impossible to carry out and evaluate the analysis. However, to demonstrate the clinical importance of these findings for breast oncology, we established an association between the mean fibre length and clinicopathological data[32] that directly influence patient survival. For this analysis, the same cut-off point defined for the analysis of the dog's survival curve (Fig. 4A) was considered. Using the cut-off point of 27 µm, women and dogs were stratified into two groups: those diagnosed with carcinomas with collagen fibres smaller than 27 µm were categorized into the first group, while those diagnosed with carcinomas with collagen fibres larger than 27 µm were grouped into the second group (Fig. 4B and I). To verify the association or independence between the mean fibre length and the clinicopathological data, we performed an analysis using the Fisher's Exact Test and the chi-square test. The data indicate that a higher proliferative rate, higher histological grade, presence of local and/or distant metastases and the "triple negative" and "Her2 overexpressed" molecular subtypes are associated with carcinomas with collagen fibres smaller than 27 µm in women (Fig. 4B, D, F and H) and dogs (Fig. 4C, E, G and I). Finally, we observed that collagen density presents an inverse correlation with histological grade (Fig. 5A and B), cell proliferation rate (Fig. 5C and D) and molecular subtype (Fig. 5E) in human breast carcinomas. Cell density has a direct correlation with molecular subtype (Fig. 5F). The same correlations were established for dogs, but no statistically significant correlations were obtained.

Discussion

Numerous studies indicate that collagen plays a key role in the tumour micro-environment, playing a critical role in the regulation of neoplastic growth and tumour cell dissemination, due to its ability to provide physical, biochemical, and biomechanical guidance for tumour and non-tumour cells[18,45–51]. Tumours can actively remodel the surrounding extracellular matrix. Type 1 and type 3 collagen fibres, when aligned, increase the stiffness of the extracellular matrix and this predicts worse outcomes[50,57] and the expression of COL11A1 may have a potential role in the aggressiveness of carcinoma in situ in women through collagen remodelling and regulation of the cellular stimulation mechanism[1]. Recent studies have described that this stiffness of the extracellular matrix is fundamental in the process of cell migration, invasion, and metastasis of tumour cel ls[18,44–49,51–65]. Here, we demonstrated that in human and canine mammary carcinomas, collagen fibres orient themselves in a preferential direction, becoming more organized.

In human mammary carcinomas, we observed that collagen fibres are more linear compared to NMTh and Fb. We did not observe this behaviour in canine mammary carcinomas. The composition of carcinomas in mixed tumours and carcinosarcomas may explain this difference. As previously stated, the MC arises from epithelial malignant transformation into benign mixed tumours[31,42,43]. It has components of malignant epithelial origin and normal or benign mesenchymal components. CS are characterized by malignant components of epithelial and mesenchymal origin, leading to intense proliferation of the extracellular matrix. MC and CS exhibit a complex histological pattern[31,33,34,36]. Thus, we noticed that canine mammary carcinomas exhibit significant heterogeneity in their composition, unlike mammary carcinomas in women, which exhibit homogeneity in epithelial and mesenchymal components. Despite exhibiting distinct features, we selected these tumours for our study because they commonly affect the female dogs, as we aim to understand the behaviour of these carcinomas in regard to the more common breast carcinomas in women.

The larger organization and alignment of collagen fibres in the tumour and peritumoural areas collected in the evaluated samples makes the stroma more rigid. We believe that this increased alignment and linearity of collagen fibres in carcinomas is associated with extracellular matrix remodelling and increased stromal stiffness. The rigid extracellular stroma, which surrounds neoplastic cells, may offer a durotactic escape route from the potentially hypoxic and necrotic environment for tumour cells. Inhospitable conditions can induce an innate mechanical sensitivity to direct cancer cells to an environment where conditions are more favourable[17,45]. The study by Toss et al., 2019[1] and Sprague et al., 2021[66] showed that the deposition and reorganization of collagen around breast carcinoma in situ plays a role in tumour progression and recurrence. The larger linearity of collagen fibres was associated with an increased risk of breast cancer recurrence in these women. Several studies show that the stiffness of the extracellular matrix and the high contractility of tumour cells severely disturb tumoural homeostasis. Matrix remodelling and cross-linking stiffens the extracellular matrix as positive feedback to further stiffen, remodel and reorient the matrix. In a transformed epithelium, increased cell tension

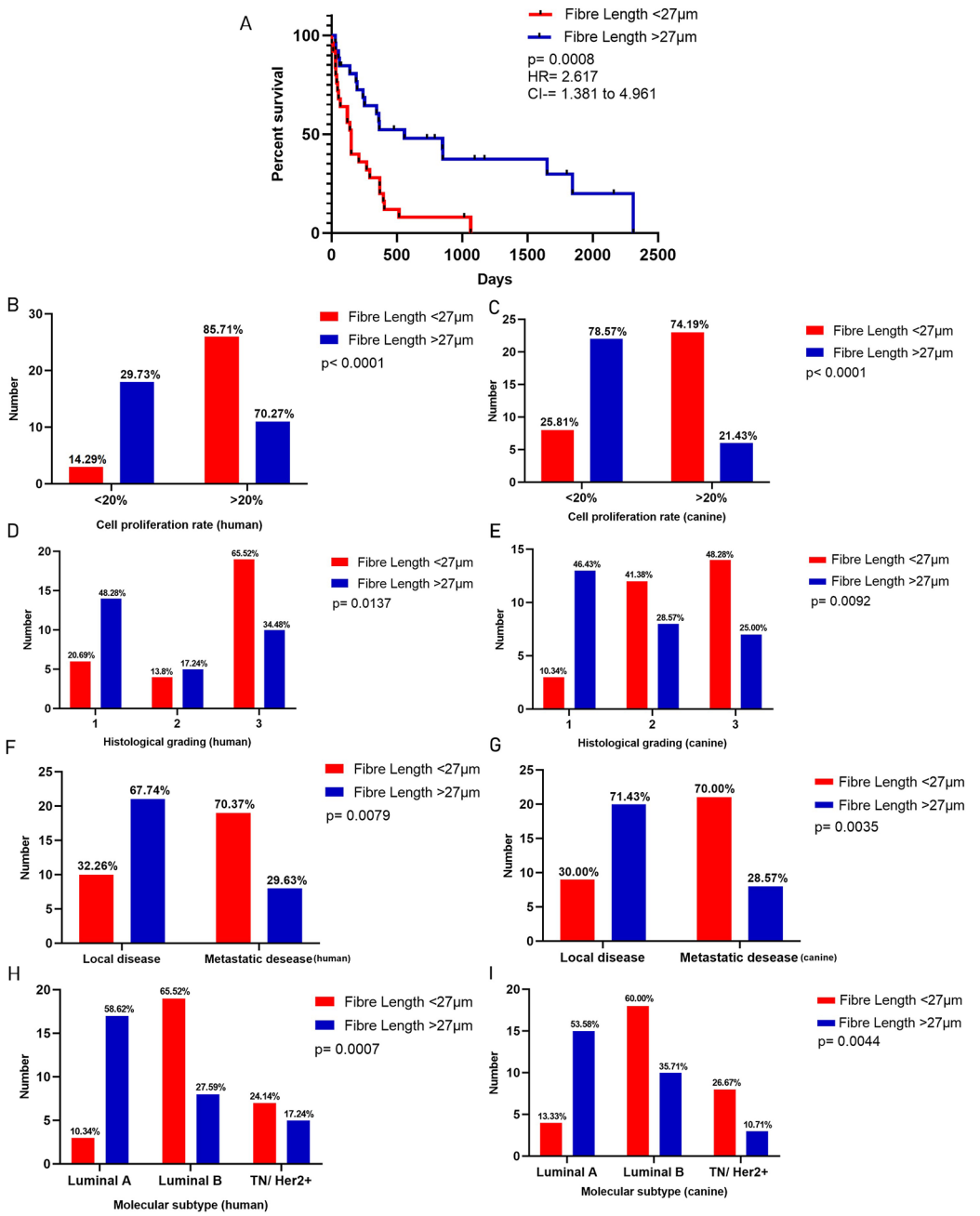

Fig. 4. Survival curve for dogs and association between clinicopathological parameters and mean fibre length in women and dogs. Kaplan–Meier curve showing the separation of cases by mean fibre length in dogs; red line for fibre length < 27 µm and blue line for fibre length > 27. (**A**, $n = 59$). Contingency plots presenting data from chi-square analysis (**D**, **E**, **H** ad **I**) and Fisher's exact test (**B**, **C**, **F** and **G**) to evaluate the association between clinicopathological data and the mean fibre length categorized in women and dogs. The clinicopathological data are presented on the x-axis, the absolute frequency (n) on the y-axis and the proportion in percentage at the end of each bar. Association between cell proliferation rate (**B**, $n = 58$), histological grade (**D**, $n = 58$), local or metastatic disease (F, $n = 58$), molecular subtype (**H**, $n = 58$) and mean fibre length categorized by the 27 µm cut-off point in women. Association between cell proliferation rate (**C**, $n = 58$), histological grade (**E**, $n = 58$), presence or absence of metastatic disease (**G**, $n = 58$) and molecular subtype (**I**, $n = 58$) and mean fibre length categorized by the cut-off point 27 µm in dogs. Error bar not included because it is the evaluation of categorical data.

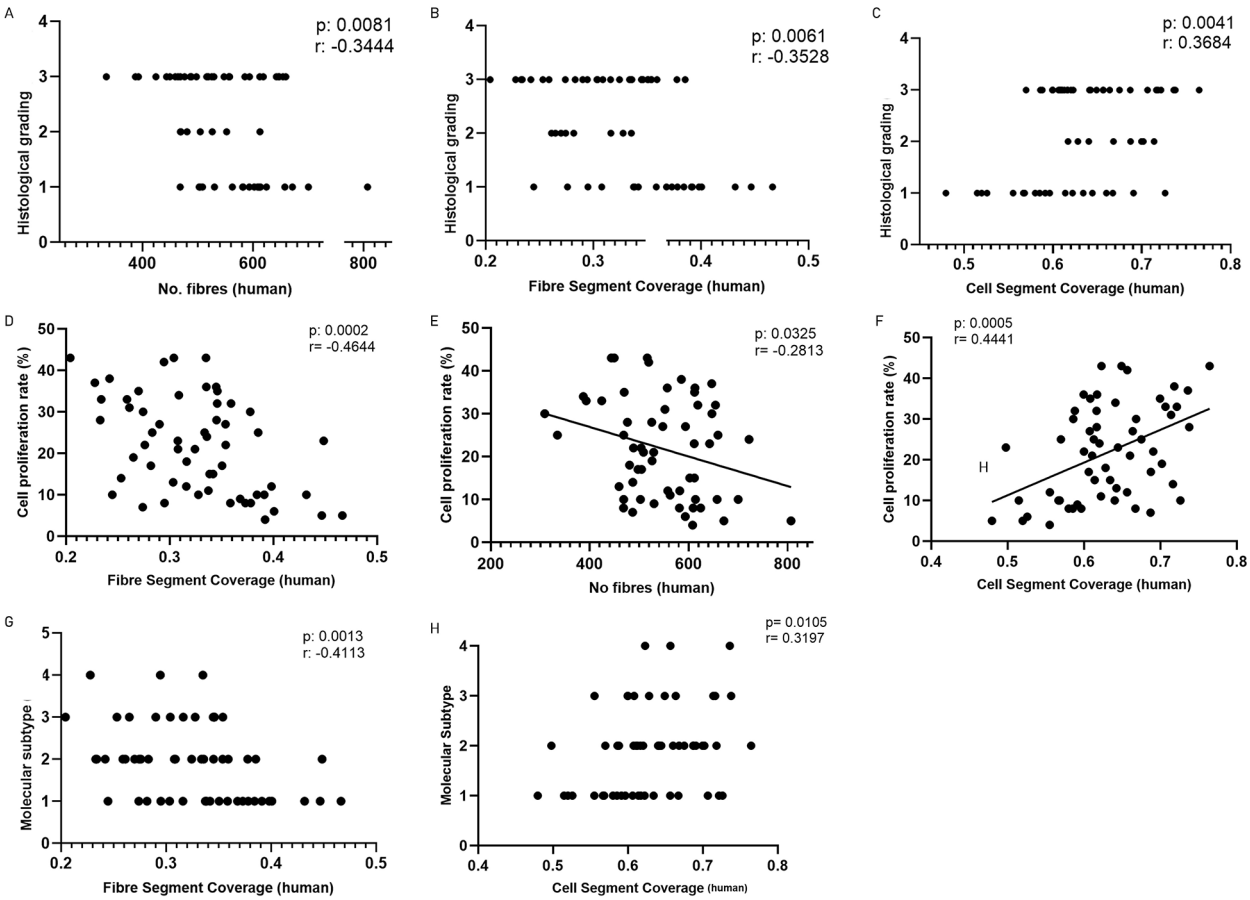

Fig. 5. Correlation between clinicopathological parameters and metrics extracted by second harmonic generation and two-photon fluorescence techniques in women. Spearman's correlation between the number of fibres (**A**, $n = 58$), fibre segment coverage (**B**, $n = 58$), cell segment coverage (**C**, $n = 58$) and histological grading. Spearman's correlation between fibre segment coverage (**G**, $n = 58$) and cell segment coverage (**H**, $n = 58$) and molecular subtype. Linear regression between the fibre segment coverage (**D**, $n = 58$), number of fibres (**E**, $n = 58$) and cell segment coverage (**F**, $n = 58$) and cell proliferation rate.

stimulates cell growth, disturbs cell-cell adhesion, compromises tissue polarity, and promotes stromal invasion by tumour cells[66–70].

We observed that in human and canine mammary carcinomas there is an exacerbated growth of epithelial components contributing to the loss of balance between stromal and parenchymal components. Therefore, the tumours present lower density of collagen fibres and higher cell density. CS does not follow this growth pattern because it has malignant epithelial and mesenchymal components. Thus, a malignant mesenchymal component induces exaggerated deposition of stromal components[31]. We therefore observed higher stromal density and lower cell density compared to other canine mammary carcinomas. In Fb, we observed higher collagen density and lower cell density compared to other histological types and NMT in humans, since the deposition of stromal elements is increased in this tumour[32].

Correlating the parameters, number of fibres, area covered by fibres and area covered by cells with the histological grade, TNM, cell proliferation rate and molecular subtype, we observed that the most aggressive human mammary carcinomas[32] present lower density of collagen fibres and higher cell density (Fig. 3). Maller et al., 2013[71] showed that the abundance of collagen in the extracellular matrix of pregnant rats was associated with reduced tumour growth and invasion compared to the tumour micro-environment of nulliparous rats. Using methods including second harmonic generation imaging, the authors showed that the abundant collagen in the mammary glands of pregnant rats is less linearised and that high-density collagen induces tumour suppressive attributes[65]. Other authors have also shown that the decrease in collagen density and increase in fibre organization is correlated with more aggressive tumour behaviour[9,62].

Another important characteristic of collagen fibres that stood out was the identification that shorter collagen fibres are associated with an unfavourable prognosis (Figs. 2F, 3A, F, A and F and 4B, I, B and I). In addition, we demonstrated that canine mammary carcinomas with shorter collagen fibres are associated with lower patient survival (Fig. 4A). Unlike women, most dogs diagnosed with mammary carcinoma are treated exclusively with surgery, without the use of chemotherapy. This fact is important to allow the study of progression of spontaneous

breast carcinomas, without the interference of chemotherapy drugs that impact the growth and development of neoplasms. Furthermore, studying mammary carcinomas in dogs avoids the bias associated with induced experimental models that are carried out within controlled environments. Thus, a comparative study using dogs as a model provides accurate data on patient survival and the behaviour of mammary carcinomas in a short period of time, since these tumours progress more quickly compared to tumours in women.

Although we were unable to plot survival curves for women, we established correlations between the number of collagen fibres, collagen fibre density, and cell density with clinicopathological data that are known to play a crucial role in patients' survival[32]. Similarly, to what occurs in the canine species, we observed that a lower number and density of fibres, a higher cell density, and shorter collagen fibres are associated with carcinomas with an unfavourable prognosis. These are important findings. It can be hypothesized that this behaviour is related to the stromal changes that occur during tumour progression, as shown in our previous work[18]. TC and ICgI in humans and MTC in dogs are carcinomas that present well-defined tubular structures, differentiated cells, low mitotic rate and low cellular and nuclear pleomorphism. The stromal component is preserved and the rate of epithelial proliferation is low. These characteristics are associated with local growth, low probability of local and/or distant metastases and favourable prognosis[31–34]. In contrast, ICgIII and IMC in humans and CS, IMC and SC in dogs present expansive growth, undifferentiated cells, high mitotic rate and high cellular and nuclear pleomorphism. The stromal component is replaced by epithelial growth because the proliferation rate of these components is high. CS does not present this behaviour because the mesenchymal component is also malignant, making it more aggressive. Thus, these carcinomas are commonly associated with local and/or distant metastases and with an unfavourable prognosis[31,32,35].

We believe that in carcinomas with a favourable prognosis and low proliferative rate, collagen fibres are larger because they limit neoplastic growth. However, in carcinomas with an unfavourable prognosis, with loss of cellular differentiation and a high proliferative rate, the collagen fibres are unable to limit this growth, and thus they rupture, allowing the tumour to expand. In this way, the fibres become fragmented and shorter compared to the fibres of carcinomas with less aggressive behaviour. Furthermore, we believe that this "shortening" of collagen fibres is associated with remodelling of the extracellular matrix to guide the metastatic invasion of tumour cells (Fig. 6). Studies show that while collagen can potentially form a protective barrier and prevent cancer cells from escaping their original location, collagen fibres also serve as a "highway" that facilitates the migration of cancer cells to remote locations, impacting survival of patients[7,9,16,62–75].

Conclusions

In conclusion, our study revealed similarities in collagen changes between human and canine mammary neoplasms, showing the association of these changes with clinicopathological factors in both species. Employing second harmonic generation, two-photon excited fluorescence techniques, and automated image analysis, we identified similar changes in the tumour stroma of human and canine mammary neoplasms. We observed that human and canine mammary carcinomas present more organized fibres. Carcinomas with higher histological grade, higher cell proliferation rate, with local and/or distant metastasis and molecular classifications of triple negative type and overexpressed Her2 present lower collagen density and higher cell density. We have also

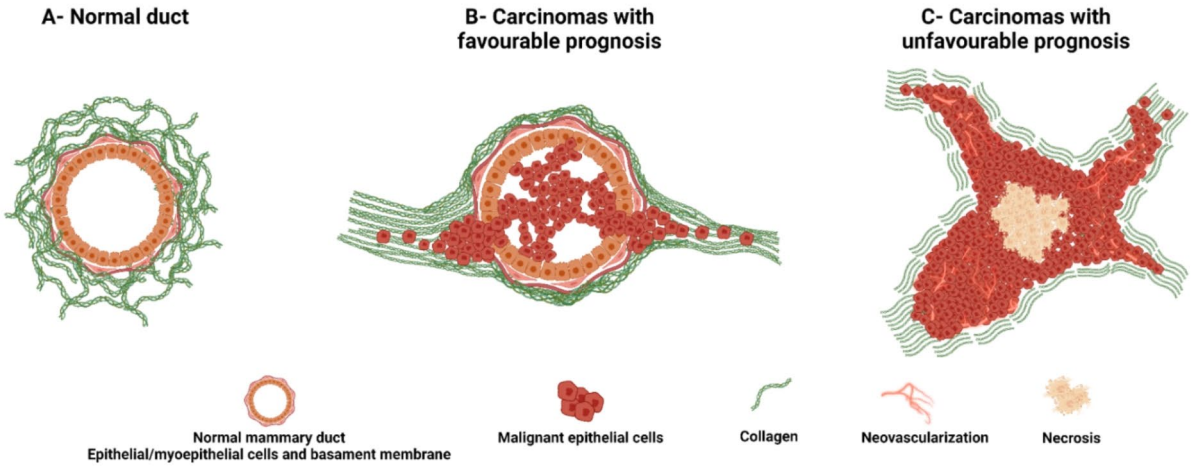

Fig. 6. Carcinomas with an unfavourable prognosis present shorter fibre. Mammary carcinomas present more organized fibres (**B** and **C**) compared to normal mammary tissue (**A**). Carcinomas with a favourable prognosis and low proliferative rate present longer collagen fibres, capable of limiting neoplastic growth (**B**). In carcinomas with an unfavourable prognosis and high proliferative rates, collagen fibres are shorter and unable to limit this growth, allowing tumour expansion (**C**). This "shortening" of collagen fibres may be associated with remodelling of the tumour stroma that creates rigid pathways to help cancer cells escape necrotic and hypoxic environments. Thus, the fibres become capable of guiding tumour cells towards locations with greater vascularization (**C**). Created by BioRender.

established a relation between the collagen fibre length and clinicopathological characteristics in women and dogs with mammary carcinomas, showing significant associations between shorter fibres and unfavourable clinical characteristics. Furthermore, we established a cut-off for the mean fibre length and specific survival time in dogs. The correlation between collagen modifications and clinicopathological factors may also have implications for diagnosis, prognosis, and the development of targeted therapies. Thus, the use of nonlinear microscopy provides new tools for assessing collagen in breast cancer.

Data availability

Data is on the link: https://mega.nz/folder/4xBylTIS#CWBOMzE-6TFRnZ3u6ys5Ig.

Received: 18 April 2024; Accepted: 12 November 2024
Published online: 21 November 2024

References

1. Toss, M. S. et al. Geometric characteristics of collagen have independent prognostic significance in breast ductal carcinoma in situ: an image analysis study. *Mod. Pathol.* **32**, 1473–1485. https://doi.org/10.1038/s41379-019-0296-7 (2019).
2. Piersma, B., Hayward, M. K. & Weaver, V. M. Fibrosis and cancer: a strained relationship. *Biochim. Biophys. Acta Rev. Cancer*. **1873** (2), 188356. https://doi.org/10.1016/j.bbcan.2020.188356 (2020).
3. Harbeck, N. et al. *Breast Cancer Nat. Rev. Dis. Primers* ; **5**:66. doi: https://doi.org/10.1038/s41572-019-0111-2. (2019).
4. Pollard, J. W. Macrophages define the invasive microenvironment in breast cancer. *J. Leukoc. Biol.* **84** (3), 623–630. https://doi.org/10.1189/jlb.1107762 (2008).
5. Markkanen, E. Know thy model: charting molecular homology in stromal reprogramming between canine and human mammary tumors. *Front. Cell. Develop Biol.* **7**, 348. https://doi.org/10.3389/fcell.2019.00348 (2019).
6. Ajeti, V. et al. Structural changes in mixed col I/Col V collagen gels probed by SHG microscopy: implications for probing stromal alterations in human breast cancer. *Biomed. Opt. Express*. **2**, 2307–2316. https://doi.org/10.1364/BOE.2.002307 (2011).
7. Conklin, M. W. et al. Aligned collagen is a prognostic signature for survival in human breast carcinoma. *Am. J. Pathol.* **178**, 1221–1232. https://doi.org/10.1016/j.ajpath.2010.11.076 (2011).
8. Garcia, A. M. et al. Second harmonic generation imaging of the collagen architecture in prostate cancer tissue. *Biomed. Phys. Eng. Express*. **4**, 025026. https://doi.org/10.1088/2057-1976/aaa379 (2017).
9. Almici, E. et al. Quantitative Image Analysis of Fibrillar Collagens Reveals Novel Diagnostic and prognostic biomarkers and histotype-dependent aberrant mechanobiology in Lung Cancer. ; **36**:100155. doi: (2023). https://doi.org/10.1016/j.modpat.2023.100155
10. Hompland, T., Erikson, A., Lindgren, M., Lindmo, T. & de Lange Davies, C. Second-harmonic generation in collagen as a potential cancer diagnostic parameter. *J. Biomed. Opt.* **13** (5), 054050. https://doi.org/10.1117/1.2983664 (2008).
11. Burke, K., Tang, P. & Brown, E. B. Second harmonic generation reveals matrix alterations during breast tumor progression. *J. Biomed. Opt.* **18**, 031106. https://doi.org/10.1117/1.JBO.18.3.031106 (2012).
12. Burke, K. et al. Using second harmonic generation to predict patient outcome in solid tumors. *BMC Cancer*. **15**, 929. https://doi.org/10.1186/s12885-015-1911-8 (2015).
13. Golaraei, A. et al. Changes of collagen ultrastructure in breast cancer tissue determined by second-harmonic generation double Stokes-Mueller polarimetric microscopy. *Biomed. Opt. Express*. **7**, 4054–4068. https://doi.org/10.1364/BOE.7.004054 (2016).
14. Barcus, C. E. et al. Elevated collagen-I augments tumor progressive signals, intravasation and metastasis of prolactin-induced estrogen receptor alpha positive mammary tumour cells. *Breast Cancer Res.* **19**, 1–13. https://doi.org/10.1186/s13058-017-0801-1 (2017).
15. Case, A. et al. Identification of prognostic collagen signatures and potential therapeutic stromal targets in canine mammary gland carcinoma. *PLoS ONE*. **12**, 1–19. https://doi.org/10.1186/s12885-015-1911-8 (2017).
16. Conklin, M. W. et al. Collagen Alignment as a predictor of recurrence after Ductal Carcinoma in situ. *Cancer Epidemiol. Biomarkers Prev.* **27** (2), 138–145. https://doi.org/10.1158/1055-9965.EPI-17-0720 (2018).
17. Reis, L. A. et al. Canine mammary cancer diagnosis from quantitative properties of nonlinear optical images. *Biomed. Opt. Express*. **11**, 6413–6427. https://doi.org/10.1364/BOE.400871 (2020).
18. Garcia, A. P. V. et al. Canine mammary cancer tumour behaviour and patient survival time are associated with collagen fibre characteristics. *Sci. Rep.* **11**, 5668. https://doi.org/10.1038/s41598-021-85104-w (2021).
19. Natal, R. A. et al. Collagen analysis by second-harmonic generation microscopy predicts outcome of luminal breast cancer. *Tumor Biol.* **40**, 1010428318770953 (2018).
20. Natal, R. A. et al. Exploring collagen parameters in pure special types of invasive breast cancer. *Sci. Rep.* **9**, 7715. https://doi.org/10.1038/s41598-019-44156-9 (2019).
21. Sorenmo, K. U. et al. The estrogen effect: clinical and histopathological evidence of dichotomous influences in dogs with spontaneous mammary carcinomas. *PLoS ONE*. **14**, e0224504. https://doi.org/10.1371/journal.pone.0224504 (2019).
22. Queiroga, F. L., Raposo, T., Carvalho, M. I., Prada, J. & Pires, I. Canine mammary tumours as a model to study human breast cancer: most recent findings. *Vivo*. **25** (3), 455–465 (2011).
23. Uva, P. et al. Comparative expression pathway analysis of human and canine mammary tumors. *BMC Genom*. **10**, 135. https://doi.org/10.1186/1471-2164-10-135 (2009).
24. Rivera, P. & Von Euler, H. Molecular biological aspects on canine and human mammary tumors. *Vet. Pathol.* **48**, 132–146. https://doi.org/10.1177/0300985810387939 (2011).
25. Markkanen, E. Know thy model: charting molecular homology in stromal reprogramming between canine and human mammary tumors. *Front. Cell. Develop Biol.* **7**, 348. https://doi.org/10.3389/fcell.2019.00348 (2019).
26. Abadie, J. et al. Canine invasive mammary carcinomas as models of human breast cancer. Part 2: immunophenotypes and prognostic significance. *Breast Cancer Res. Treat.* **167**, 459–468. https://doi.org/10.1007/s10549-017-4542-8 (2018).
27. Gray, M. et al. Naturally-occurring canine mammary tumors as a translational model for human breast cancer. *Front. Oncol.* **10**, 617. https://doi.org/10.3389/fonc.2020.00617 (2020).
28. Nguyen, B. N., Moriarty, R. A., Kamalitdinov, T., Etheridge, J. M. & Fisher, J. P. Collagen hydrogel scaffold promotes mesenchymal stem cell and endothelial cell coculture for bone tissue engineering. *J. Biomed. Mater. Res. A*. **105** (4), 1123–1131. https://doi.org/10.1002/jbm.a.36008 (2017).
29. D. Cassali, G. Comparative mammary oncology: canine model. *BMC Proc.* **7** (K6). https://doi.org/10.1186/1753-6561-7-S2-K6 (2013).
30. Owen, L. N. & World Health Organization. Veterinary Public Health Unit and WHO Collaborating Center for Comparative Oncology. &. TNM classification of tumours in domestic animals, edited by L.N. Owen (1980). https://apps.who.int/iris/handle/10665/68618
31. Goldschmidt, M., Peña, L., Rasotto, R. & Zappulli, V. Classification and grading of canine mammary tumors. *Vet. Pathol.* **48** (1), 117–131. https://doi.org/10.1177/0300985810393258 (2011).

32. Peña, L., De Andrés, P. J., Clemente, M., Cuesta, P. & Pérez-Alenza, M. D. Prognostic value of histological grading in noninflammatory canine mammary carcinomas in a prospective study with two-year follow-up: relationship with clinical and histological characteristics. *Vet. Pathol.* **50** (1), 94–105. https://doi.org/10.1177/0300985812447830 (2013).
33. Nunes, F. C. et al. The prognostic significance of immunophenotypes in canine malignant mammary tumors. *Arq. Bras. Med. Vet. Zootec.* **74**, 2. https://doi.org/10.1590/1678-4162-12273 (2022).
34. Cassali, G. D. et al. Canine mammary mixed tumours: a review. *Vet. Med. Int.* **1–7**, 274608. https://doi.org/10.1155/2012/274608 (2012).
35. Gamba, C. et al. Histopathological and immunohistochemical assessment of invasive micropapillary mammary carcinoma in dogs: a retrospective study. *Vet. J.* **196**, 241–246. https://doi.org/10.1016/j.tvjl.2012.08.022 (2013).
36. Damasceno, K. A. et al. Relationship between the expression of versican and EGFR, HER-2, HER-3 and CD44 in matrix-producing tumours in the canine mammary gland. Histol. Histopathol. Cell. Mol. Biol. 31:675 – 88 (2016). doi: (2016). https://doi.org/10.14670/HH-11-705
37. World Health Organization. Classification of Tumors. Breast Cancer. 5th ed.
38. Nakagaki, K. Y. R. et al. Solid Carcinoma of the Canine Mammary Gland: a histological type or Tumour Cell Arrangement? *J. Comp. Pat.* **190**, 1–12. https://doi.org/10.1016/j.jcpa.2021.10.011 (2022).
39. Gomes, E. F. et al. Prostate cancer tissue classification by multiphoton imaging, automated image analysis and machine learning. *J. Biophotonics*. **16** (6), e202200382. https://doi.org/10.1002/jbio.202200382 (2023).
40. Longford, F. G. & Pyfibre Python fibrous image analysis toolkit. https://github.com/franklongford/PyFibre, (2023). Version 2.1.1.
41. Garcia, A. P. V., Taborda, D. Y. O., Reis, L. A., de Paula, A. M. & Cassali, G. D. Collagen modifications predictive of lymph node metastasis in dogs with carcinoma in mixed tumours. *Front. Vet. Sci.* **11**, 1362693. https://doi.org/10.3389/fvets.2024.1362693 (2024).
42. Moulton, J. E., Taylor, D. O. N., Dorn, C. R. & Andersen, A. C. *Canine Mammary Tumors Vet. Pat.* ; **7**:4. doi: https://doi.org/10.1177/030098587000700401. (1970).
43. Misdorp, W. Histological classification of the mammary tumors of the dog and the cat. World Health Organ. Int. Histol. Classif. Tumors Domestic Anim. 2ª ed. (1999).
44. Ouellette, J. N. et al. Navigating the Collagen Jungle: the Biomedical potential of Fiber Organization in Cancer. *Bioengineering*. **8**, 17. https://doi.org/10.3390/bioengineering8020017 (2021).
45. DuChez, B. J., Doyle, A. D., Dimitriadis, E. K. & Yamada, K. M. Durotaxis by human cancer cells. *Biophys. J.* **116**, 670–683. https://doi.org/10.1016/j.bpj.2019.01.009 (2019).
46. Toss, M. S. et al. Collagen (XI) alpha-1 chain is an independent prognostic factor in breast ductal carcinoma in situ. *Mod. Pat.* **32**, 1460–1472. https://doi.org/10.1038/s41379-019-0286-9 (2019).
47. Mierke, C. T. The pertinent role of cell and matrix mechanics in Cell Adhesion and Migration. *Front. Cell. Dev. Biol.* **9**, 720494. https://doi.org/10.3389/fcell.2021.720494 (2021).
48. Moriyama, K. & Kidoaki, S. Cellular Durotaxis revisited: initial-position-dependent determination of the threshold stiffness gradient to induce durotaxis. *Langmuir*. **35**, 7478–7486. https://doi.org/10.1021/acs.langmuir.8b02529 (2018).
49. Zhang, K. et al. The collagen receptor discoidin domain receptor 2 stabilizes SNAIL1 to facilitate breast cancer metastasis. *Nat. Cell. Biol.* **15**, 677–687 (2013).
50. Souza, F. P. et al. Development and characterization of poultry collagen-based hybrid hydrogels for bone regeneration. *Acta Cir. Bras.* **37**, 3. https://doi.org/10.1590/acb370302 (2022).
51. Weigelin, B. & Friedl, P. A three-dimensional organotypic assay to measure target cell killing by cytotoxic T lymphocytes. *Biochem. Pharmacol.* **80** (12), 2087–2091. https://doi.org/10.1016/j.bcp.2010.09.004 (2010).
52. Bredfeldt, J. S. et al. Computational segmentation of collagen fibres from second-harmonic generation images of breast cancer. *J. Biomed. Opt.* **19**, 016007. https://doi.org/10.1117/1.JBO.19.1.016007 (2014).
53. Tuer, A. E. et al. Nonlinear optical properties of type I collagen fibres studied by polarization dependent second harmonic generation microscopy. *J. Phys. Chem. B.* **115**, 12759–12769. https://doi.org/10.1021/jp206308k (2011).
54. Burke, K., Tang, P. & Brown, E. Second harmonic generation reveals matrix alterations during breast tumor progression. *J. Biomed. Opt.* **18**, 031106. https://doi.org/10.1117/1.JBO.18.3.031106 (2012).
55. Brabrand, A. et al. Alterations in collagen fibre patterns in breast cancer. A premise for tumour invasiveness? APMIS. ; **123**:1–8. doi: (2015). https://doi.org/10.1111/apm.12298
56. Hall, M. S. et al. Fibrous nonlinear elasticity enables positive mechanical feedback between cells and ECMs. Proc. Natl. Acad. Sci. 113:14043–14048. doi: (2016). https://doi.org/10.1073/pnas.1613058113
57. Barcus, C. E. & Longmore, G. D. Collagen linearization within tumors. *Cancer Res.* **81** (22), 5611–5612. https://doi.org/10.1158/0008-5472.CAN-21-2939 (2021).
58. Guo, S. & Deng, C. X. Effect of stromal cells in tumor microenvironment on metastasis initiation. Int. J. Biol. Sci. ; 14:2083. doi: (2018). https://doi.org/10.7150/ijbs.25720
59. Wang, K. et al. Breast cancer cells alter the dynamics of stromal fibronectin–collagen interactions. *Matrix Biol.* **60–61**, 86–95. https://doi.org/10.1016/j.matbio.2016.08.001 (2017).
60. Rezakhaniha, R. et al. Experimental investigation of collagen waviness and orientation in the arterial adventitia using confocal laser scanning microscopy. *Biomech. Model. Mechanobiol.* **11**, 461–473. https://doi.org/10.1007/s10237-011-0325-z (2012).
61. Ávila, F. J. & Bueno, J. M. Analysis and quantification of collagen organization with the structure tensor in second harmonic microscopy images of ocular tissues. *Appl. Opt.* **54**, 9848–9854. https://doi.org/10.1364/AO.54.009848 (2015).
62. Brett, E. A., Sauter, M. A., Machens, H. G. & Duscher, D. Tumor-associated collagen signatures: pushing tumor boundaries. *Can. Metab.* **8**, 14. https://doi.org/10.1186/s40170-020-00221-w (2020).
63. Xu, S. et al. The role of collagen in cancer: from bench to bedside. *J. Translational Med.* **17**, 309. https://doi.org/10.1186/s12967-019-2058-1 (2019).
64. Gole, L. et al. Quantitative stain-free imaging and digital profiling of collagen structure reveal diverse survival of triple negative breast cancer patients. *Breast Cancer Res.* **22**, 42. https://doi.org/10.1186/s13058-020-01282-x (2020).
65. Cox, T. R. The matrix in cancer Thomas R. Cox. *Nat. Rev. Can.* **21**, 217–238. https://doi.org/10.1038/s41568-020-00329-7 (2021).
66. Sprague, B. L. et al. Collagen organization in relation to ductal carcinoma in situ pathology and outcomes. *Cancer Epidemiol. Biomarkers Prev.* **30** (1), 80–88. https://doi.org/10.1158/1055-9965.EPI-20-0889 (2021).
67. Wu, Y. H., Chou, C. Y. & Collagen, X. I. Alpha 1 chain, a Novel Therapeutic Target for Cancer Treatment. *Front. Oncol.* **12**, 925165. https://doi.org/10.3389/fonc.2022.925165 (2022).
68. Song, K. et al. Collagen remodeling along Cancer Progression providing a Novel Opportunity for Cancer diagnosis and treatment. *Int. J. Mol. Sci.* **23** (18), 10509. https://doi.org/10.3390/ijms231810509 (2022).
69. Huang, J. et al. Extracellular matrix and its therapeutic potential for cancer treatment. *Sig Transd Targ Ther.* **6**, 153. https://doi.org/10.1038/s41392-021-00544-0 (2021).
70. Ogunniyan, W. J., Metcalf, A. A. & Werb, K. J. Concepts of extracellular matrix remodelling in tumour progression and metastasis. *Nat. Comm.* **11**, 5120. https://doi.org/10.1038/s41467-020-18794-x (2020).
71. Maller, O. et al. Collagen architecture in pregnancy-induced protection from breast cancer. *J. Cell. Sci.* **126**, 4108–4110. https://doi.org/10.1242/jcs.121590 (2013).
72. Provenzano, P. P. et al. Collagen reorganization at the tumor-stromal interface facilitates local invasion. *BMC Med.* **4** (1), 38. https://doi.org/10.1186/1741-7015-4-38.PMID (2006).

73. Provenzano, P. P. et al. Collagen density promotes mammary tumor initiation and progression. *BMC Med.* **28**, 611. https://doi.org/10.1186/1741-7015-6-11 (2008).
74. Giorello, M. B., Borzone, F. R., Labovsky, V., Piccioni, F. V. & Chasseing, N. A. Cancer-associated fibroblasts in the breast tumor microenvironment. *J. Mammary Gl Biol. Neoplasia.* **26** (2), 135–155. https://doi.org/10.1007/s10911-020-09475-y (2021).
75. Bourgot, I., Primac, I., Lois, T., Noel, A. & Maquoi, E. Reciprocal interplay between Fibrillar Collagens and collagen-binding integrins: implications in Cancer Progression and Metastasis. *Front. Oncol.* **10** https://doi.org/10.3389/fonc.2020.01488 (2020).

Author contributions
APVG selected and prepared the samples, analysed the patients' clinical and pathological data, selected the fields for data acquisition in SHG and TPEF imaging, performed the immunohistochemistry technique and marker analysis, prepared the figures and tables, and drafted the manuscript. BRMR participated in acquisition and analysis of SHG and TPEF image data and image analysis of human samples. LAR participated in the acquisition and analysis of SHG and TPEF image data and image analysis of canine samples. CBN participated in the selection of human samples. GDC and AMdP guided APVG throughout all project phases, reviewed and edited the manuscript. GDC participated in the selection of canine samples and reviewed the clinical-pathological and immunohistochemical data. AMdP supervised all stages of SHG and TPEF data acquisition and image analysis. All authors read and approved the final paper.

Funding
This work was supported by Fundação de Amparo à Pesquisa do Estado de Minas Gerais (FAPEMIG) [Rede Mineira de Pesquisa Translacional em Imunobiológicos e Biofármacos no Câncer (REMITRIBIC, RED-00031-21)]; Conselho Nacional de Desenvolvimento Científico e Tecnológico (CNPq) and Coordenação de Aperfeiçoamento de Pesssoal de Nível Superior (Capes), Brazil.

Declarations

Ethics approval and consent to participate
The canine sample study was performed in view of the fundamental ethical principles under law no. 11.794, of October 8, 2008 and of decree no. 6.899 of July 2009, and with the rules issued by the National Council for the Control of Animal Experimentation (CONCEA) and the international Animal Research: Reporting of In Vivo Experiments (ARRIVE). All experimental protocols were approved by the "Ethics Committee on the Use of Animals" at UFMG, under number 83/2021. The research on human tissue sample was previously approved by the "Research Ethics Committee" at UFMG (COEP-UFMG) under No. 43947521.3.0000.5149/2021.
All experiments were carried out in accordance with the Declaration of Helsinki. As a retrospective study, performed on archive histopathological slides, the need for informed consent from all subjects and/or their legal guardian(s) was waived by the COEP-UFMG.

Consent for publication
Not applicable.

Competing interests
The authors declare no competing interests.

Additional information
Supplementary Information The online version contains supplementary material available at https://doi.org/10.1038/s41598-024-79854-6.

Correspondence and requests for materials should be addressed to A.M.P.